**5268** *J. Phys. Chem. A* **2004,** *108,* 5268−5277

# Theoretical Investigation of the Potential Energy Surface of the $Si_2NP$ Molecule

**Guang-hui Chen,[†,‡] Yi-hong Ding,*[,†] Xu-ri Huang,[†] Ze-sheng Li,[†] and Chia-chung Sun[†]**

*State Key Laboratory of Theoretical and Computational Chemistry, Institute of Theoretical Chemistry, Jilin University, Changchun 130023, People's Republic of China and Department of Chemistry, Mudanjiang Normal College, Mudanjiang 157012, People's Republic of China*

*Received: January 17, 2004; In Final Form: March 31, 2004*

The structures, energetics, spectroscopies, and stabilities of the singlet and triplet $Si_2NP$ isomeric species are explored at the DFT/B3LYP, QCISD, and CCSD(T) (single-point) levels. A total of 23 minimum isomers and 32 interconversion transition states are located. Generally, the triplet species lie energetically higher than the singlet ones. At the CCSD(T)/6-311+G(2df)//QCISD/6-311G(d) level, there are two nearly isoenergetic singlet isomers as global minima, i.e., a linear SiNSiP $^1$**1** (0.0) and a puckered cSiNSiP $^1$**4** with P−N cross-bonding (−0.6). The third low-lying isomer is a planar four-membered ring cSiNSiP $^1$**5** (3.3) with Si−Si cross-bonding. All the three isomers have reasonable kinetic stabilities and might be observable either in laboratory or in space. Moreover, the structural and bonding analyses indicate that $^1$**1** possesses typical Si≡P triple bonding. Since up to now, stable Si≡P triply bonded species are still experimentally unknown, isomer $^1$**1** may represent such a good example. Finally, the similarities and discrepancies of $Si_2NP$ are compared to the other analogous 18-valence electrons species AA′BB′ (A, A′ are group IV elements and B, B′ are group V elements) such as $C_2N_2$ and $Si_2P_2$. The present study is the first one to consider such series with three higher-row atoms.

## 1. Introduction

Recently, the nitrogen, silicon, and phosphorus-related chemistries have received considerable attention in various fields. For example, they have important applications in microelectronic materials and surface chemistry. Silicon clusters doping group V elements are commonly used as semiconductor materials. Another interesting field is interstellar chemistry. Up to now, many species containing N, Si, and P have been found in space.[1]

There have been many studies on the binary clusters $Si_nN_m$[2] and $Si_nP_m$[3](mainly theoretical). However, there has been little attention on the ternary clusters $Si_nN_mP_o$, even for the simplest SiNP molecule. Investigations of such ternary species may offer useful insights toward understanding the properties of N,P-doped $Si_n$ materials. In this paper, we report our work on the tetra-atomic cluster $Si_2NP$, which is chemically isovalent to the well-known $C_2N_2$ molecule,[4] as well as other species $C_2NP$,[5] $SiCN_2$,[6] $Si_2N_2$[7], and $Si_2P_2$.[8] All these molecules have singlet linear ground structures except $Si_2P_2$, whose ground state is a puckered form with P−P cross-bonding followed by a planar rhombic structure with Si−Si cross-bonding. $Si_2NP$ is formally the intermediate between $Si_2N_2$ and $Si_2P_2$. Generally, the first-row atoms prefer to form $\pi$-bonds, while the second-row atoms prefer to form $\sigma$-bonds. So it is interesting to see (1) the relative stabilities of linear and cyclic species (planar or puckered) may contribute to (2) whether $Si_2NP$ has stable isomers that contain triple bonds between the second-row elements, i.e., Si≡Si and Si≡P, and (3) whether the triplet potential energy surface is important or not. A detailed theoretical study can resolve such kinds of problems. On the basis of our knowledge of the tetra-atomic AA′BB′ (A, A′ are group IV elements and B, B′ are group V elements) series with 18 valence electrons, the present study on $Si_2NP$ containing three higher-row atoms may represent the first study and may contribute to the understanding of the structural and bonding changes upon heterodoping.

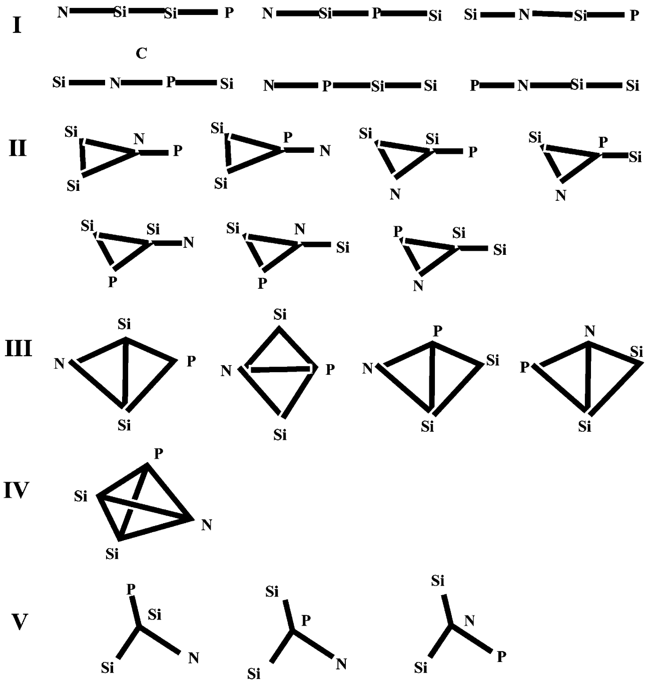

**Figure 1.** The scheme for the singlet and triplet $Si_2NP$ isomeric species search that follows.

## 2. Computational Methods

All computations are carried out using the GAUSSIAN98[9] program package. The optimized geometries and harmonic vibrational frequencies of the local minima and transition

---

* To whom correspondence should be addressed.
[†] Jilin University.
[‡] Mudanjiang Normal College.

10.1021/jp049747s CCC: \$27.50

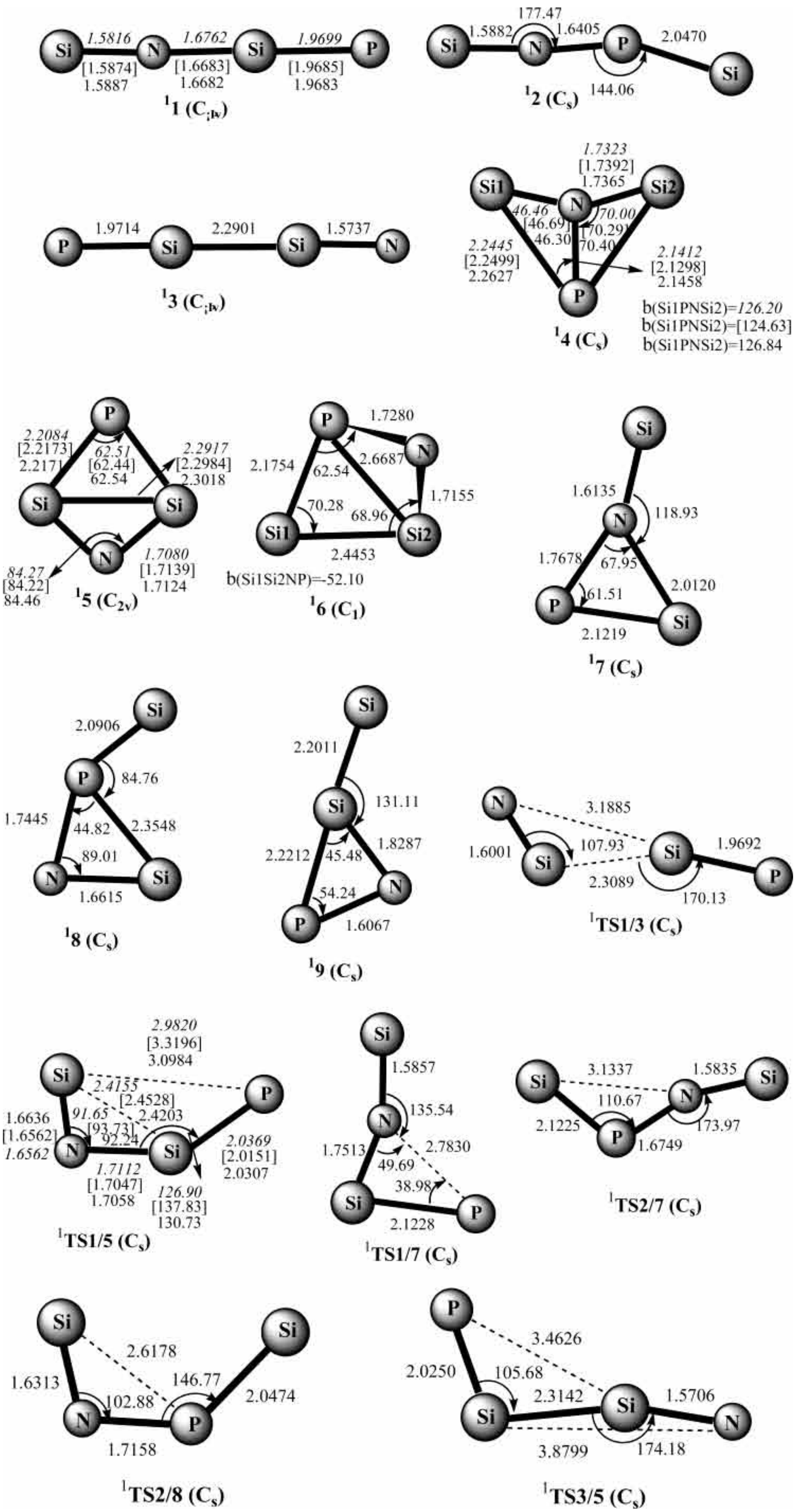
Si N Si P
1.5816 1.6762 1.9699
[1.5874] [1.6683] [1.9685]
1.5887 1.6682 1.9683
$^1$1 ($C_{;lv}$)
Si N P Si
1.5882 177.47 1.6405 2.0470 144.06
$^1$2 ($C_s$)
P Si Si N
1.9714 2.2901 1.5737
$^1$3 ($C_{;lv}$)
Si1 N Si2 P
1.7323 [1.7392] 1.7365
46.46 [46.69] 46.30
70.00 [70.29] 70.40
2.2445 [2.2499] 2.2627
2.1412 [2.1298] 2.1458
b(Si1PNSi2)=126.20
b(Si1PNSi2)=[124.63]
b(Si1PNSi2)=126.84
$^1$4 ($C_s$)
P Si Si N
2.2084 [2.2173] 2.2171
62.51 [62.44] 62.54
2.2917 [2.2984] 2.3018
84.27 [84.22] 84.46
1.7080 [1.7139] 1.7124
$^1$5 ($C_{2v}$)
P N Si1 Si2
1.7280 2.1754 62.54 2.6687 70.28 68.96 1.7155 2.4453
b(Si1Si2NP)=-52.10
$^1$6 ($C_1$)
Si N P Si
1.6135 118.93 1.7678 67.95 61.51 2.0120 2.1219
$^1$7 ($C_s$)
Si P N Si
2.0906 84.76 1.7445 44.82 2.3548 89.01 1.6615
$^1$8 ($C_s$)
Si Si N P
2.2011 131.11 2.2212 45.48 1.8287 54.24 1.6067
$^1$9 ($C_s$)
N Si Si P
3.1885 1.6001 107.93 1.9692 2.3089 170.13
$^1$TS1/3 ($C_s$)
Si N Si P
2.9820 [3.3196] 3.0984
2.4155 [2.4528] 2.4203
1.6636 [1.6562] 1.6562
91.65 [93.73] 92.24
1.7112 [1.7047] 1.7058
2.0369 [2.0151] 2.0307
126.90 [137.83] 130.73
$^1$TS1/5 ($C_s$)
Si N Si P
1.5857 135.54 1.7513 2.7830 49.69 38.98 2.1228
$^1$TS1/7 ($C_s$)
Si N P Si
3.1337 1.5835 110.67 2.1225 173.97 1.6749
$^1$TS2/7 ($C_s$)
Si N P Si
2.6178 146.77 1.6313 102.88 2.0474 1.7158
$^1$TS2/8 ($C_s$)
P Si Si N
3.4626 2.0250 105.68 2.3142 1.5706 3.8799 174.18
$^1$TS3/5 ($C_s$)

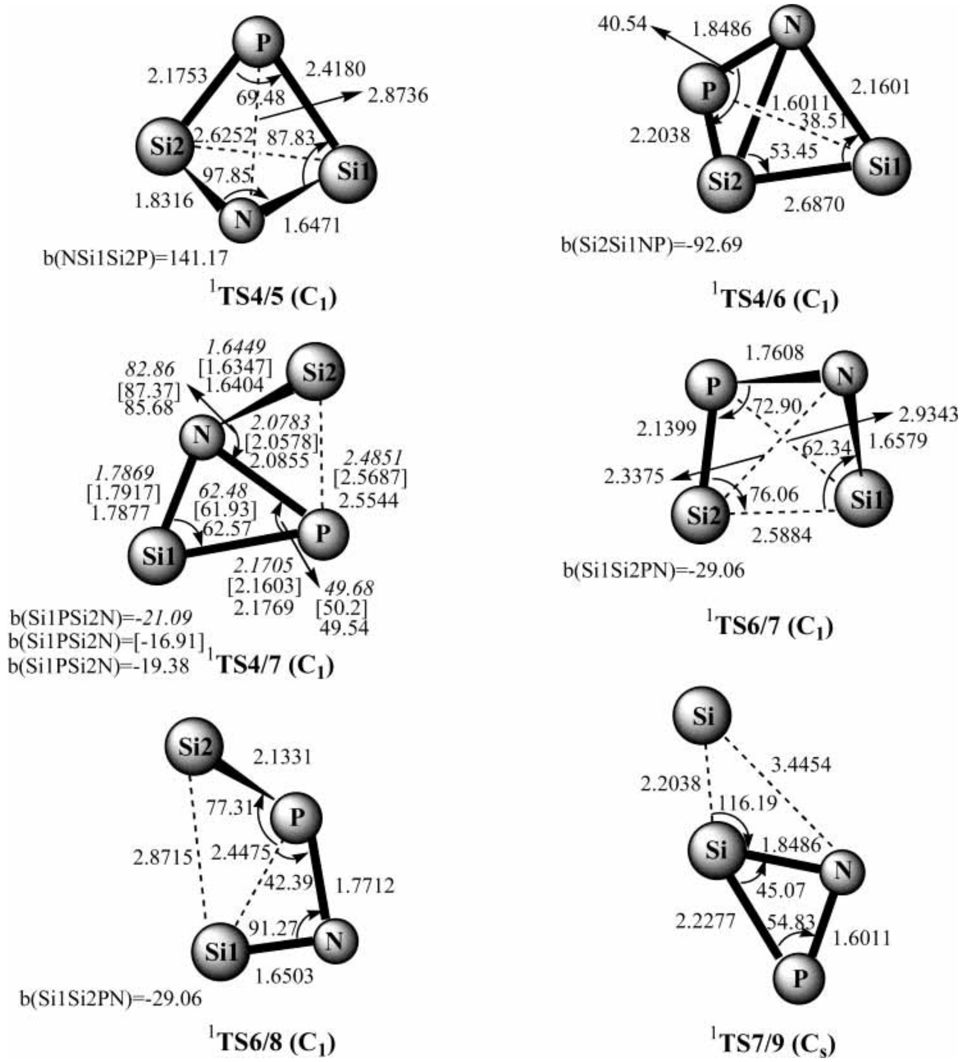

**Figure 2.** Optimized geometries of singlet $Si_2NP$ isomers and transition states at the DFT/B3LYP/6-311G(d) level and the geometrical parameters in italics and brackets at the QCISD/6-311G(d) and DFT/B3LYP/cc-pVTZ levels, respectively. Bond lengths are in angstroms, and angles are in degrees.

states are obtained at the DFT/B3LYP/6-311G(d) theory level. Moreover, single-point calculations are performed at the CCSD(T)/6-311G(2df) level using the DFT/B3LYP/6-311G(d) optimized geometries. The DFT/B3LYP/6-311G(d) zero-point vibration energies (ZPVE) are also included. To confirm whether the obtained transition states connect with the right isomers, intrinsic reaction coordinate (IRC) calculations are performed at the DFT/B3LYP/6-311G(d) level. Finally, the geometries and energies of the relevant species are more accurately calculated at the DFT/B3LYP/cc-pVTZ, QCISD/6-311G(d), single-point CCSD(T)/cc-pVTZ//DFT/B3LYP/cc-pVTZ and CCSD(T)/6-311+G(2df)//QCISD/6-311G(d) levels, respectively.

## 3. Results and Discussions

For the tetra-atomic $Si_2NP$ molecule, we considered various isomeric forms as many as possible, which include five types of isomers, i.e., linear or chainlike species (I), three-membered ring species (II), four-membered ring species (III), closed species (IV), and branched-chain species (V), as depicted in Figure 1. After numerous searches, a total of 23 $Si_2NP$ minimum isomers (9 for singlet and 14 for triplet) ($^s$**m**) and 32 interconversion transition states (12 for singlet and 20 for triplet) ($^s$**TSm/n**) were obtained at the DFT/B3LYP/6-311G(d) level. Note that the top left corner number **s** means the electronic state (1 for singlet and 3 for triplet) of the isomers or transition states. The calculated structures of various singlet and triplet $S_2NP$ species are shown in Figures 2 and 3, respectively, and those of the fragments are shown in Figure 4. The calculated spectroscopic properties (harmonic vibrational frequencies, rotational constants, and dipole moments) of $Si_2NP$ are given in Table 1. The energetic properties of $Si_2NP$ species and fragments are listed in Tables 2 and 3, respectively. Finally, the schematic potential energy surfaces (PESs) showing the isomerization and dissociation of $Si_2NP$ are presented in Figure 5 (for singlet) and Figure 6 (for triplet).

**3.1. Singlet PES of $Si_2NP$.** The nine singlet isomers are of the chainlike, three-membered and four-membered ring forms as shown in Figure 2. Interestingly, there are two isomers with almost the same energy, i.e., the linear SiNSiP $^1$**1** and the puckered cSiNSiP $^1$**4** with N−P cross-bonding. As indicated in Table 2, the 6-311G(d) used DFT/B3LYP and QCISD methods predict $^1$**1** to be more stable than $^1$**4** by about 8.5 and 9.7 kcal/mol, respectively. Yet, higher-level CCSD(T)/6-311G(2df) and CCSD(T)/6-311+G(2df) calculations using both DFT/B3LYP and QCISD geometries put $^1$**1** and $^1$**4** energetically rather close, with the difference being just 0.4 and −0.6 kcal/mol, respectively. The additional CCSD(T)/cc-pVTZ//DFT/B3LYP/

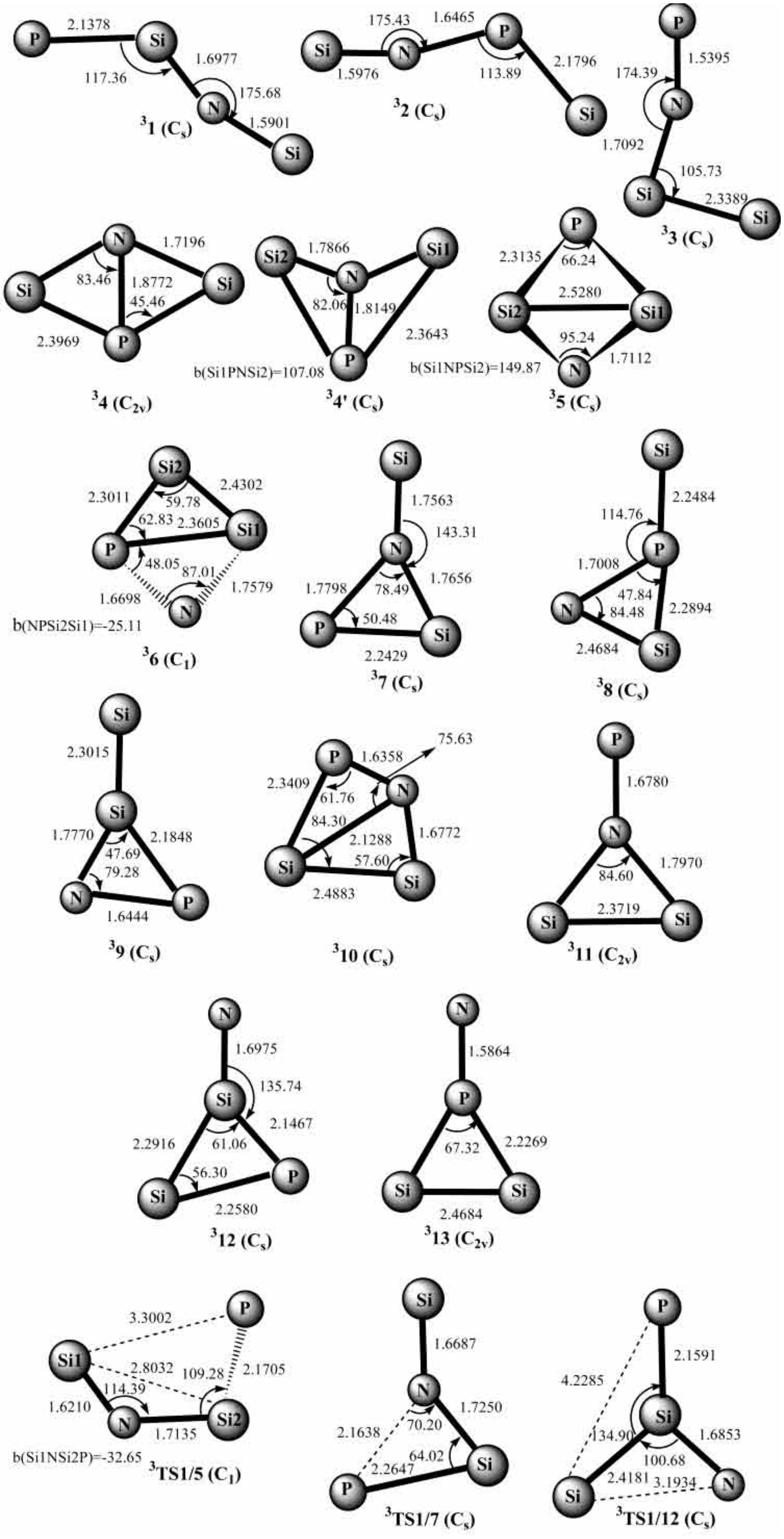
P 2.1378 Si 117.36 1.6977 175.68 N 1.5901 Si
$^{3}$1 ($C_s$)
Si 1.5976 175.43 N 1.6465 P 113.89 2.1796 Si
$^{3}$2 ($C_s$)
P 1.5395 174.39 N 1.7092 105.73 Si 2.3389 Si
$^{3}$3 ($C_s$)
N 1.7196 Si 83.46 1.8772 45.46 Si 2.3969 P
$^{3}$4 ($C_{2v}$)
Si2 1.7866 N Si1 82.06 1.8149 2.3643 P b(Si1PNSi2)=107.08
$^{3}$4' ($C_s$)
P 2.3135 66.24 Si2 2.5280 Si1 95.24 N 1.7112 b(Si1NPSi2)=149.87
$^{3}$5 ($C_s$)
Si2 2.3011 2.4302 59.78 62.83 2.3605 P Si1 48.05 87.01 1.6698 1.7579 N b(NPSi2Si1)=-25.11
$^{3}$6 ($C_1$)
Si 1.7563 N 143.31 1.7798 78.49 1.7656 P 50.48 Si 2.2429
$^{3}$7 ($C_s$)
Si 2.2484 114.76 P 1.7008 47.84 N 84.48 2.2894 2.4684 Si
$^{3}$8 ($C_s$)
Si 2.3015 Si 1.7770 2.1848 47.69 79.28 N P 1.6444
$^{3}$9 ($C_s$)
P 1.6358 75.63 2.3409 61.76 N 84.30 2.1288 1.6772 Si 57.60 Si 2.4883
$^{3}$10 ($C_s$)
P 1.6780 N 1.7970 84.60 Si 2.3719 Si
$^{3}$11 ($C_{2v}$)
N 1.6975 Si 135.74 2.1467 2.2916 61.06 56.30 Si P 2.2580
$^{3}$12 ($C_s$)
N 1.5864 P 2.2269 67.32 Si Si 2.4684
$^{3}$13 ($C_{2v}$)
3.3002 P Si1 2.8032 109.28 2.1705 1.6210 114.39 N 1.7135 Si2 b(Si1NSi2P)=-32.65
$^{3}$TS1/5 ($C_1$)
Si 1.6687 N 1.7250 2.1638 70.20 64.02 Si P 2.2647
$^{3}$TS1/7 ($C_s$)
P 2.1591 4.2285 Si 134.90 1.6853 100.68 2.4181 3.1934 Si N
$^{3}$TS1/12 ($C_s$)

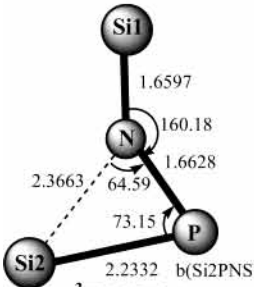

**$^3$TS2/7 $(C_1)$**

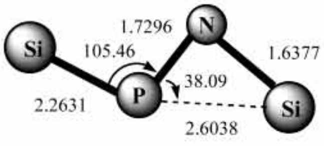

**$^3$TS2/8 $(C_s)$**

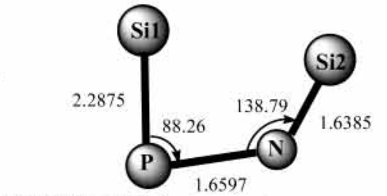

**$^3$TS2/10 $(C_1)$**

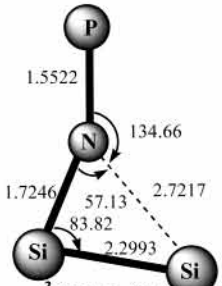

**$^3$TS3/11 $(C_s)$**

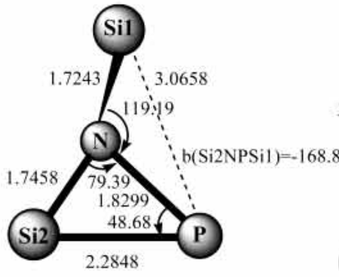

**$^3$TS4/7 $(C_1)$**

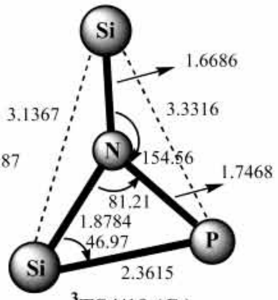

**$^3$TS4/10 $(C_s)$**

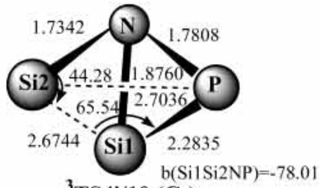

**$^3$TS4'/10 $(C_1)$**

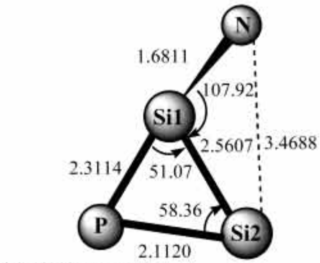

**$^3$TS5/12 $(C_1)$**

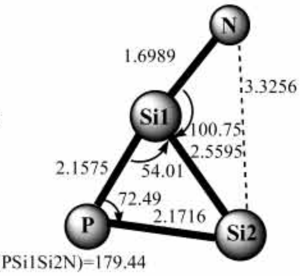

**$^3$TS5/12* $(C_1)$**

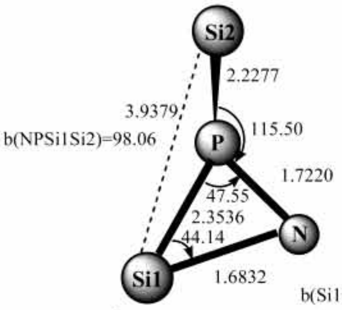

**$^3$TS6/8 $(C_1)$**

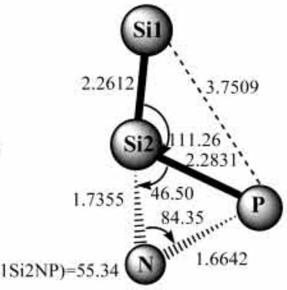

**$^3$TS6/9 $(C_1)$**

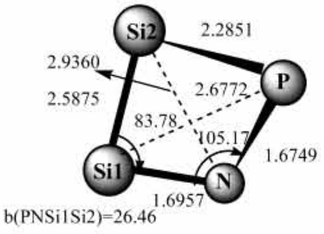

**$^3$TS6/10 $(C_1)$**

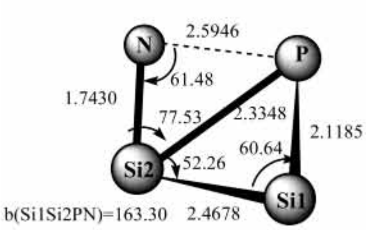

**$^3$TS6/12 $(C_1)$**

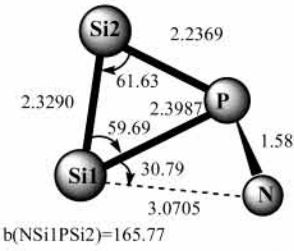

**$^3$TS6/13 $(C_1)$**

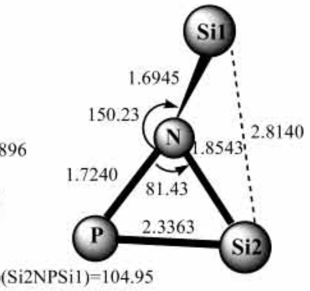

**$^3$TS7/10 $(C_1)$**

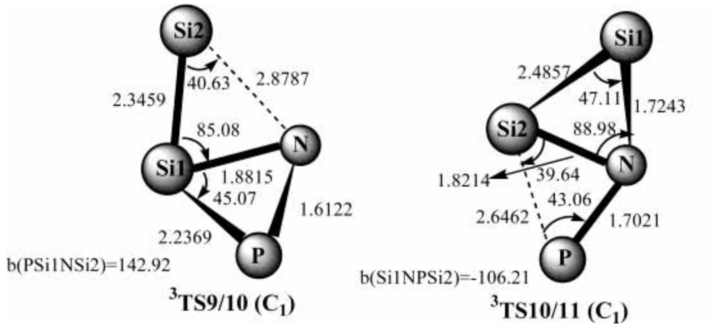

$^3$**TS9/10 (C$_1$)** $^3$**TS10/11 (C$_1$)**

**Figure 3.** Optimized geometries of triplet $Si_2NP$ isomers and transition states at the DFT/B3LYP/6-311G(d) level. Bond lengths are in angstroms, and angles are in degrees.

**TABLE 1: Harmonic Vibrational Frequencies (cm$^{-1}$), Infrared Intensities (km/mol) (in parentheses), Dipole Moment (D), and Rotational Constants (GHz) of Singlet and Triplet $Si_2NP$ Structures at the DFT/B3LYP/6-311G(d) Level**

| species | frequencies (infrared intensity) | dipole moments | rotational constants |
|---|---|---|---|
| SiNSiP $^1$**1** ($^1\Sigma$) | 85(0) 85(0) 230(11) 230(11) 445(2) 824(6) 1347(292) | 5.7037 | 1.182544 |
| SiNSiP $^1$**1** ($^1\Sigma$)$^a$ | 74(1) 74(1) 214(10) 214(10) 444(11) 826(16) 1384(466) | 5.4384 | 1.180799 |
| SiNSiP $^1$**1** ($^1\Sigma$)$^b$ | 85(1) 85(1) 216(6) 216(6) 444(2) 825(2) 1342(239) | 5.4750 | 1.182978 |
| SiPNSi $^1$**2** ($^1A'$) | 48(4) 223(4) 227(10) 450(22) 709(10) 1304(111) | 2.2014 | |
| PSiSiN $^1$**3** ($^1\Sigma$) | 45(4) 45(4) 85(14) 85(14) 296(0) 751(1) 1221(0) | 3.1819 | |
| cSiPSiN $^1$**4** ($^1A'$) | 235(4) 319(27) 395(7) 427(52) 713(24) 824(50) | 1.4099 | 6.50035, 3.93814, 2.67506 |
| cSiPSiN $^1$**4** ($^1A'$)$^a$ | 235(4) 332(30) 400(16) 440(42) 735(21) 853(57) | 1.4566 | 6.56207, 3.99396, 2.71631 |
| cSiPSiN $^1$**4** ($^1A'$)$^b$ | 244(3) 338(28) 391(11) 444(41) 721(22) 822(49) | 1.0780 | 6.52204, 3.98370, 2.71927 |
| cSiPSiN $^1$**5** ($^1A_1$) | 214(1) 305(24) 479(1) 535(35) 642(6) 886(73) | 0.1882 | 6.81965, 4.31441, 2.64259 |
| cSiPSiN $^1$**5** ($^1A_1$)$^a$ | 202(1) 309(25) 490(0) 550(34) 650(7) 904(65) | 0.3305 | 6.88022, 4.34093, 2.66163 |
| cSiPSiN $^1$**5** ($^1A_1$)$^b$ | 231(0) 306(19) 485(0) 542(31) 651(6) 887(67) | 0.5340 | 6.83883, 4.30435, 2.64168 |
| cSiSiPN $^1$**6** | 252(18) 295(3) 307(18) 503(3) 710(26) 797(10) | 1.7020 | |
| Si-cNPSi $^1$**7** ($^1A'$) | 101(3) 280(17) 314(29) 441(4) 602(16) 1131(2) | 1.6970 | |
| Si-cPSiN $^1$**8** ($^1A'$) | 66(4) 148(1) 341(19) 515(36) 682(91) 946(8) | 2.4265 | |
| Si-cSiPN $^1$**9** ($^1A'$) | 15(0) 71(4) 336(8) 507(14) 599(19) 1005(61) | 1.7926 | |
| SiNSiP $^3$**1** ($^3A'$) | 87(2) 182(14) 252(13) 477(3) 614(36) 1306(305) | 3.8697 | |
| SiNPSi $^3$**2** ($^3A'$) | 100(2) 240(17) 269(7) 453(7) 589(2) 1254(128) | 2.1800 | |
| PNSiSi $^3$**3** ($^3A'$) | 64(1) 265(9) 268(5) 379(9) 550(3) 1210(294) | 1.9412 | |
| SiPSiN $^3$**4** ($^3B_2$) | 217(7) 260(12) 292(0) 510(41) 637(41) 923(133) | 0.3410 | |
| SiPSiN $^3$**4′** ($^3A'$) | 207(1) 218(1) 354(24) 544(19) 636(23) 738(32) | 0.2713 | |
| cSiPSiN $^3$**5** ($^3A''$) | 198(12) 244(1) 332(2) 409(29) 785(0) 803(30) | 1.1086 | |
| cSiSiPN $^3$**6** | 257(7) 268(5) 365(9) 434(17) 661(0) 821(53) | 1.5433 | |
| Si-cNSiP $^3$**7** ($^3A''$) | 132(0) 168(0) 357(9) 508(38) 575(15) 970(238) | 1.5525 | |
| Si-cPSiN $^3$**8** ($^3A''$) | 41(1) 100(5) 284(5) 470(41) 714(67) 872(19) | 1.9874 | |
| Si-cSiNP $^3$**9** | 61(1) 89(2) 307(5) 516(14) 686(17) 941(26) | 1.9338 | |
| cSiSiPN $^3$**10** ($^3A'$) | 20(6) 245(9) 342(2) 436(93) 629(27) 1067(3) | 0.4005 | |
| P-cNSiSi $^3$**11** ($^3A_2$) | 128(0) 235(3) 360(0) 522(0) 567(6) 880(39) | 0.2569 | |
| N-cSiSiP $^3$**12** ($^3A''$) | 121(8) 140(15) 342(7) 410(3) 511(6) 823(117) | 2.4413 | |
| N-cPSiSi $^3$**13** ($^3A_2$) | 118(3) 138(8) 294(5) 385(1) 430(10) 893(44) | 3.1083 | |

[a] At the QCISD/6-311G(d) level. [b] At the DFT/B3LYP/cc-pVTZ level.

cc-pVTZ calculations predict the relative energy of $^1$**4** to be −0.4 kcal/mol above $^1$**1**. Within the computational errors, we consider $^1$**1** and $^1$**4** to be isoenergetic species. At the DFT/B3LYP/6-311G(d) level, the outer SiN bond value 1.5887 Å of SiNSiP $^1$**1** is close to the typical Si═N double bonds (1.6004 Å from $H_2Si{=}NH$[10]). Its SiP bond value 1.9683 Å is also very close to that of the typical Si≡P triple bond (1.9570 Å from HSi≡P). Isomer $^1$**1** can be described with a valence structure |Si═N−Si≡P|, which is consistent with the orbital analysis. Like the analogous 18-valence electron species CNCN, CNCP, SiNCN, etc., SiNSiP $^1$**1** has two sets of delocalized $\pi$-orbitals with the most weight on internal Si−N bonding, and has two sets of localized $\pi$-orbitals within Si−N and Si−P bonding with the former bearing very weak $\pi$-overlap. As a result, the shorter inner SiN bond (1.6682 Å), compared to the typical Si−N single bond value 1.7283 Å in $SiH_3NH_2$, is due to the delocalized $\pi$-orbitals**.** The bent isomer SiNPSi $^1$**2** (19.3) and the linear PSiSiN $^1$**3** (72.1) are much higher in energy. This can be rationalized that, for SiN and SiP radicals, the valence structures |Si═N|$^\bullet$ and $^\bullet$Si≡P| have greater weights than $^\bullet$Si≡N| and |Si═P|$^\bullet$, respectively. All the species $^1$**1**, $^1$**2**, and $^1$**3** can be thought of as adducts between SiN and SiP radicals. The form SiPSiN is not a minimum. Note that the value in parentheses are relative energies in kcal/mol at the CCSD(T)//DFT/B3LYP level, unless specified.

The low-lying puckered form cSiNSiP $^1$**4** has a long crossed N−P bond (2.1458 Å), compared to the normal NP single bond (1.7172 Å in $NH_2PH_2$). Such weak N−P cross-bonding decreases the strain with the two cNSiP rings and contributes to the stabilization of the puckered $^1$**4**. The peripheral SiN (1.7365 Å) and SiP (2.2627 Å) bonds are close to the typical Si−N single bond (1.7283 Å) and Si−P single bond (2.2820 Å). The four-membered ring isomer cSiNSiP $^1$**5** has a planar $C_{2v}$ symmetry. The crossed Si−Si (2.3018 Å), peripheral SiN (1.7124 Å), and SiP (2.2171 Å) bonds are close to but slightly shorter than the typical Si−Si (2.3547 Å in $H_3SiSiH_3$), Si−N, and Si−P single bonds. This is caused by one set of delocalized $\pi$-orbital. There is one additional set of $\pi$ antibonding orbitals between N and P. Therefore, isomer $^1$**5** can be considered as a singlet diradical. Such a property is similar to that

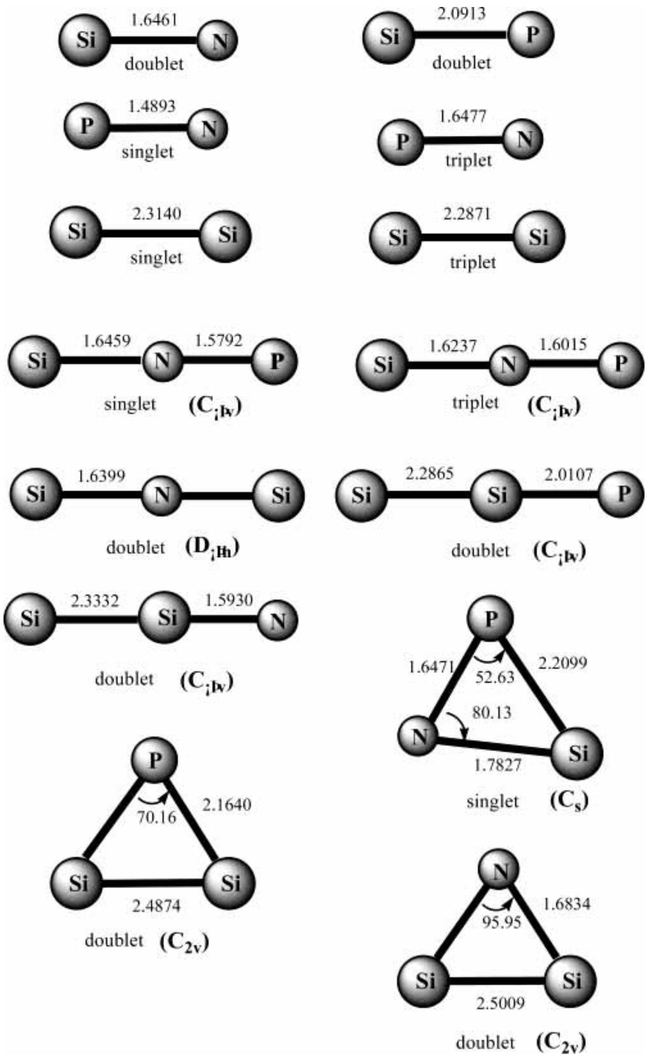

**Figure 4.** Optimized fragments of the dissociations of $Si_2NP$ at the DFT/B3LYP/6-311G(d) level. Bond lengths are in angstroms, and angles are in degrees.

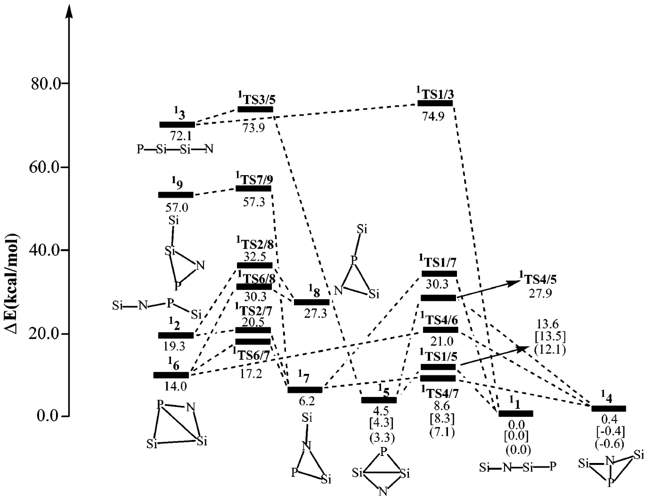

**Figure 5.** Schematic singlet potential-energy surface of $Si_2NP$ at the CCSD(T)/6-311G(2df)//DFT/B3LYP/6-311G(d)+ZPVE level. The relative energies in parentheses and brackets are at the CCSD(T)/6-311+G-(2df)//QCISD/6-311G(d)+ZPVE and CCSD(T)/cc-pVTZ// DFT/B3LYP/cc-pVTZ levels, respectively.

of the analogous $Si_2N_2$ and $Si_2P_2$ species. At the CCSD(T)//QCISD+ZPVE level, isomer $^{1}$**5** is the third low-lying form at 3.3 kcal/mol. Isomer $^{1}$**6** (14.0) can be viewed as a puckered four-membered species with a weak Si−P cross single bonding (2.6687 Å). Finally, there are three isomers Si-cNPSi $^{1}$**7** (6.2), Si-cSiNP $^{1}$**8** (27.3), and Si-cSiPN $^{1}$**9** (57.0) that contain three-membered rings.

To judge the observable possibilities of $Si_2NP$ isomers, consideration of the isomerization and dissociation stabilities is very important. Table 3 indicates that all the isomers are stable against dissociation. So the isomerization shown in Figure 5 governs the kinetic stability of singlet $Si_2NP$ isomers. For simplicity, the transition state details are omitted. The least isomerization barrier order for the nine isomers is listed as follows: $^{1}$**1**(13.6, *12.1*, $^{1}$**1** → $^{1}$**5**) > $^{1}$**5**(9.1, *8.8*, $^{1}$**5** → $^{1}$**1**) > $^{1}$**4**(8.2, *7.7*, $^{1}$**4** → $^{1}$**7**) > $^{1}$**6**(3.2, $^{1}$**6** → $^{1}$**7**) > $^{1}$**8**(3.0, $^{1}$**8** → $^{1}$**6**) > $^{1}$**7**(2.4, $^{1}$**7** → $^{1}$**4**) > $^{1}$**3**(1.8, $^{1}$**3** → $^{1}$**5**) > $^{1}$**2**(1.2, $^{1}$**2** → $^{1}$**7**) > $^{1}$**9**(0.3, $^{1}$**9** → $^{1}$**7**). The italic values are at the CCSD(T)//QCISD level. We can find that the isomers $^{1}$**1,** $^{1}$**4**, and $^{1}$**5** are of most interest. Besides being the three low-lying isomers, $^{1}$**1,** $^{1}$**4**, and $^{1}$**5** have reasonable kinetic stabilities and could be observable either in interstellar space or in the laboratory. Note that the direct conversion transition state between the two isoenergetic species $^{1}$**1** and $^{1}$**4** cannot be located. Instead, such attempts always lead to the low-lying $^{1}$**TS4/7,** which connects the puckered cSiNSiP $^{1}$**4** and the three-membered ring Si-cNPSi $^{1}$**7**.

**3.2. Triplet PES of $Si_2NP$.** There are 14 triplet $Si_2NP$ isomers (structures shown in Figure 3). Among them, three isomers SiNSiP $^{3}$**1**(23.2), SiNPSi $^{3}$**2**(42.6), and PNSiSi $^{3}$**3**(60.6) are of chainlike type. Five isomers, i.e., planar cSiNSiP $^{3}$**4**(18.4) with N−P cross-bonding, puckered cSiNSiP $^{3}$**4′**(29.9) with N−P cross-bonding, cSiNSiP $^{3}$**5**(17.8) with Si−Si cross-bonding, cSiNPSi $^{3}$**6**(33.1) with Si−P cross-bonding, and cSiNPSi $^{3}$**10**(21.6) with N−Si cross-bonding, are four-membered ring species. The remaining six species Si-cNPSi $^{3}$**7** (30.1), Si-cPNSi $^{3}$**8** (55.2), Si-cSiPN $^{3}$**9** (57.9), P-cNSiSi $^{3}$**11** (29.1), N-cSiSiP $^{3}$**12** (66.6), N-cPSiSi $^{3}$**13** (72.1) have three-membered rings. All the triplet isomers have higher energies than the corresponding singlet ones. From the triplet PES (Figure 6) containing 20 transition states, the kinetic stability order for the triplet isomers is $^{3}$**10**(14.1,$^{3}$**10** → $^{3}$**11**) > $^{3}$**5**(13.1, $^{3}$**5** → $^{3}$**1**) > $^{3}$**4**(12.5, $^{3}$**4** → $^{3}$**7**) > $^{3}$**6**(10.9, $^{3}$**6** → $^{3}$**10**) > $^{3}$**9**(9.8, $^{3}$**9** → $^{3}$**10**) > $^{3}$**13**(7.9, $^{3}$**13** → $^{3}$**6**) > $^{3}$**1**(7.7, $^{3}$**1** → $^{3}$**5**) > $^{3}$**11**(6.6, $^{3}$**11** → $^{3}$**10**) > $^{3}$**12**(6.2, $^{3}$**12** → $^{3}$**6**) > $^{3}$**2**(3.6, $^{3}$**2** → $^{3}$**10**) > $^{3}$**8** (2.7, $^{3}$**8** → $^{3}$**6**) > $^{3}$**3**(2.4, $^{3}$**3** → $^{3}$**11**) = $^{3}$**4′**(2.4, $^{3}$**4′** → $^{3}$**10**) > $^{3}$**7**(0.8, $^{3}$**7** → $^{3}$**4**). At the CCSD(T)//B3LYP level, the singlet−triplet gaps of $^{1}$**1**, $^{1}$**4**, and $^{1}$**5** are determined to be 23.2, 18.0, and 13.3 kcal/mol, respectively.

It is of interest to investigate the validity of the computational approaches used in the present paper. The calculated spectroscopic properties (in Table 1) and the structures (in Figure 2) of the most relevant species $^{1}$**1**, $^{1}$**4**, $^{1}$**5**, $^{1}$**TS1/5**, and $^{1}$**TS4/7** at the DFT/B3LYP//6-311G(d) level are very close to those at the DFT/B3LYP/cc-pVTZ level. Also, their CCSD(T)/6-311G(2df)//DFT/B3LYP/6-311G(d) relative energies (in Table 2) are very close to the CCSD(T)/cc-pVTZ//DFT/B3LYP/cc-pVTZ values. Thus, the one-particle basis sets 6-311G(d) and 6-311+G(2df) are enough for prediction of the geometries, spectroscopies, and energies, respectively. Moreover, the correlational methods have minor importance because the 6-311G(d)-based DFT/B3LYP and QCISD structures, spectroscopies, and energies are similar. However, increasing the size of the basis set is important in dertermining the energies.

On the other hand, we explore the effects of the monodeterminantal methods for such Si, P-containing systems, especially for the singlet diradical isomer $^{1}$**5**. We calculated the diagnostic factors $\tau_1$ for the isomers $^{1}$**1**, $^{1}$**4**, and $^{1}$**5** at the CCSD(T)/6-311G-(2df) level, which are 0.027, 0.025, and 0.027, respectively. So

**TABLE 2: Relative (kcal/mol) Energies of the Singlet and Triplet $Si_2NP$ Isomers and Transition States at the DFT/B3LYP/6-311G(d) and Single-Point CCSD(T)/6-311g(2df) Levels**[a]

| species | B3LYP$^c$ | ΔZPVE B3LYP$^c$ | CCSD(T)$^d$ //B3LYP$^c$ | total 1 | QCISD$^c$ | ΔZPVE QCISD$^c$ | CCSD(T)$^e$ //QCISD$^c$ | total 2 | B3LYP$^f$ | ΔZPVE B3LYP$^f$ | CCSD(T)$^f$ //B3LYP$^f$ | total 3 |
|---|---|---|---|---|---|---|---|---|---|---|---|---|
| SiNSiP $^{1}$**1**$^{b}$ ($^{1}\Sigma$) | 0.0 | 0.0 | 0.0 | 0.0 | 0.0 | 0.0 | 0.0 | 0.0 | 0.0 | 0.0 | 0.0 | 0.0 |
| SiPNSi $^{1}$**2** ($^{1}A'$) | 19.0 | −0.4 | 19.7 | 19.3 | | | | | | | | |
| PSiSiN $^{1}$**3** ($^{1}\Sigma$) | 79.1 | −1.0 | 73.1 | 72.1 | | | | | | | | |
| cSiPSiN $^{1}$**4** ($^{1}A'$) | 8.5 | −0.5 | 0.9 | 0.4 | 9.7 | −0.3 | −0.3 | −0.6 | 3.3 | −0.4 | 0.0 | −0.4 |
| cSiPSiN $^{1}$**5** ($^{1}A_1$) | 15.7 | −0.3 | 4.8 | 4.5 | 18.4 | −0.2 | 3.5 | 3.3 | 8.4 | −0.2 | 4.5 | 4.3 |
| cSiSiPN $^{1}$**6** | 23.0 | −0.5 | 14.5 | 14.0 | | | | | | | | |
| Si-cNPSi $^{1}$**7** ($^{1}A'$) | 7.9 | −0.5 | 6.7 | 6.2 | | | | | | | | |
| Si-cPSiN $^{1}$**8** ($^{1}A'$) | 37.7 | −0.8 | 28.1 | 27.3 | | | | | | | | |
| Si-cSiPN $^{1}$**9** ($^{1}A'$) | 62.5 | −1.0 | 58.0 | 57.0 | | | | | | | | |
| $^{1}$TS**1/3** ($^{1}A'$) | 83.5 | −1.3 | 76.2 | 74.9 | | | | | | | | |
| $^{1}$TS**1/5** ($^{1}A'$) | 21.6 | −0.4 | 14.0 | 13.6 | 23.1 | −0.3 | 12.4 | 12.1 | 16.5 | −0.3 | 13.8 | 13.5 |
| $^{1}$TS**1/7** ($^{1}A'$) | 29.6 | −0.9 | 31.2 | 30.3 | | | | | | | | |
| $^{1}$TS**2/7** ($^{1}A'$) | 19.7 | −0.6 | 21.1 | 20.5 | | | | | | | | |
| $^{1}$TS**2/8** ($^{1}A'$) | 38.6 | −1.0 | 33.5 | 32.5 | | | | | | | | |
| $^{1}$TS**3/5** ($^{1}A'$) | 82.2 | −1.2 | 75.1 | 73.9 | | | | | | | | |
| $^{1}$TS**4/5** | 37.4 | −1.0 | 28.9 | 27.9 | | | | | | | | |
| $^{1}$TS**4/6** | 30.7 | −1.1 | 22.1 | 21.0 | | | | | | | | |
| $^{1}$TS**4/7** | 13.4 | −0.8 | 9.4 | 8.6 | 14.2 | −0.7 | 7.8 | 7.1 | 10.4 | −0.7 | 9.0 | 8.3 |
| $^{1}$TS**6/7** | 24.7 | −0.9 | 18.1 | 17.2 | | | | | | | | |
| $^{1}$TS**6/8** | 39.8 | −1.1 | 31.4 | 30.3 | | | | | | | | |
| $^{1}$TS**7/9** ($^{1}A'$) | 62.6 | −1.0 | 58.3 | 57.3 | | | | | | | | |
| SiNSiP $^{3}$**1** ($^{3}A'$) | 20.5 | −0.5 | 23.7 | 23.2 | | | | | | | | |
| SiNPSi $^{3}$**2** ($^{3}A'$) | 39.3 | −0.5 | 43.1 | 42.6 | | | | | | | | |
| PNSiSi $^{3}$**3** ($^{3}A'$) | 53.9 | −0.7 | 61.3 | 60.6 | | | | | | | | |
| SiPSiN $^{3}$**4** ($^{3}B_2$) | 19.7 | −0.6 | 19.0 | 18.4 | | | | | | | | |
| SiPSiN $^{3}$**4′** ($^{3}A'$) | 34.9 | −0.8 | 30.7 | 29.9 | | | | | | | | |
| cSiPSiN $^{3}$**5** ($^{3}A''$) | 23.4 | −0.7 | 18.5 | 17.8 | | | | | | | | |
| cSiSiPN $^{3}$**6** | 40.5 | −0.6 | 33.7 | 33.1 | | | | | | | | |
| Si-cNSiP $^{3}$**7** ($^{3}A''$) | 28.4 | −0.8 | 30.9 | 30.1 | | | | | | | | |
| Si-cPSiN $^{3}$**8** ($^{3}A''$) | 57.0 | −1.0 | 56.2 | 55.2 | | | | | | | | |
| Si-cSiNP $^{3}$**9** ($^{3}A''$) | 62.2 | −0.9 | 58.8 | 57.9 | | | | | | | | |
| cSiSiPN $^{3}$**10** ($^{3}A'$) | 23.7 | −0.7 | 22.3 | 21.6 | | | | | | | | |
| P-cNSiSi $^{3}$**11** ($^{3}A_2$) | 27.8 | −0.8 | 29.9 | 29.1 | | | | | | | | |
| N-cSiSiP $^{3}$**12** ($^{3}A''$) | 67.9 | −1.3 | 67.9 | 66.6 | | | | | | | | |
| N-cPSiSi $^{3}$**13** ($^{3}A_2$) | 75.2 | −1.4 | 73.5 | 72.1 | | | | | | | | |
| $^{3}$TS**1/5** | 32.7 | −0.9 | 31.8 | 30.9 | | | | | | | | |
| $^{3}$TS**1/7** ($^{3}A''$) | 35.2 | −1.4 | 40.0 | 38.6 | | | | | | | | |
| $^{3}$TS**1/12** ($^{3}A'$) | 115.1 | −2.1 | 122.0 | 119.9 | | | | | | | | |
| $^{3}$TS**2/7** | 45.9 | −1.2 | 52.2 | 51.0 | | | | | | | | |
| $^{3}$TS**2/8** ($^{3}A''$) | 59.0 | −1.4 | 60.2 | 58.8 | | | | | | | | |
| $^{3}$TS**2/10** | 45.0 | −1.0 | 47.2 | 46.2 | | | | | | | | |
| $^{3}$TS**3/11** ($^{3}A'$) | 55.5 | −1.0 | 64.0 | 63.0 | | | | | | | | |
| $^{3}$TS**4/7** | 30.7 | −1.2 | 32.1 | 30.9 | | | | | | | | |
| $^{3}$TS**4/10** ($^{3}A'$) | 38.1 | −1.2 | 43.4 | 42.2 | | | | | | | | |
| $^{3}$TS**4′/10** | 37.0 | −1.1 | 33.4 | 32.3 | | | | | | | | |
| $^{3}$TS**5/12** | 81.3 | −1.8 | 79.2 | 77.4 | | | | | | | | |
| $^{3}$TS**5/12*** | 83.3 | −1.8 | 82.8 | 81.0 | | | | | | | | |
| $^{3}$TS**6/8** | 59.4 | −1.2 | 59.1 | 57.9 | | | | | | | | |
| $^{3}$TS**6/9** | 69.5 | −1.5 | 69.5 | 68.0 | | | | | | | | |
| $^{3}$TS**6/10** | 48.7 | −1.2 | 45.2 | 44.0 | | | | | | | | |
| $^{3}$TS**6/12** | 76.4 | −1.9 | 74.7 | 72.8 | | | | | | | | |
| $^{3}$TS**6/13** | 84.7 | −2.0 | 82.0 | 80.0 | | | | | | | | |
| $^{3}$TS**7/10** | 32.8 | −1.3 | 38.8 | 37.5 | | | | | | | | |
| $^{3}$TS**9/10** | 70.1 | −1.6 | 69.3 | 67.7 | | | | | | | | |
| $^{3}$TS**10/11** | 35.6 | −1.4 | 37.1 | 35.7 | | | | | | | | |

[a] For the relevant species, the values at the CCSD(T)/6-311+G(2df)//QCISD/6-311G(d) and CCSD(T)/cc-pVTZ//DFT/B3LYP/cc-pVTZ levels are listed also. The symbols in parentheses of the column denote the point group symmetry. [b] The total energies of reference isomer $^{1}$**1** at the DFT/B3LYP/6-311G(d) level is −975.1323410 au, at the CCSD(T)/6-311G(2df)//DFT/B3LYP/6-311G(d) level is −973.6300628 au, at the QCISD/6-311G(d) level is −973.4878341 au, and at the CCSD(T)/6-311+G(2df)/QCISD/6-311G(d) level is −973.6336544 au, respectively. The ZPVE at the DFT/B3LYP and QCISD levels are 0.007391 and 0.007360 au, respectively. [c] The basis set is 6-311G(d) for DFT/B3LYP and QCISD. [d] The basis set is 6-311G(2df) for the CCSD(T). [e] The 6-311+G(2df) basis set is used for CCSD(T). [f] The cc-pVTZ basis set is used.

the nondynamical effects are of minute importance, and the monodeterminantal approach is adequate for description of $Si_2NP$.

**3.3 Comparison with Analogous Species.** It is desirable to compare $Si_2NP$ with the isovalent species such as $C_2N_2$,[4] $C_2NP$,[5] $SiCN_2$,[6] $Si_2N_2$,[7] and $Si_2P_2$,[8] which have been previously studied. For $C_2N_2$, $C_2NP$, $SiCN_2$ that contain none or one second-row atom (Si or P), the linear species are thermodynamically and kinetically more stable and no four-membered ring species are of interest. The latter two species each contain two or more than two second-row atoms. For $Si_2N_2$, the linear isomers SiNNSi and SiNSiN are the first and third low-lying species. A puckered one cSiNSiN with N−N cross-bonding is energetically the second most stable.[11] For $Si_2P_2$, the lowest energy isomer is a singlet butterfly-like structure with P−P cross-bonding followed by a singlet rhombic SiPSiP isomer with Si−

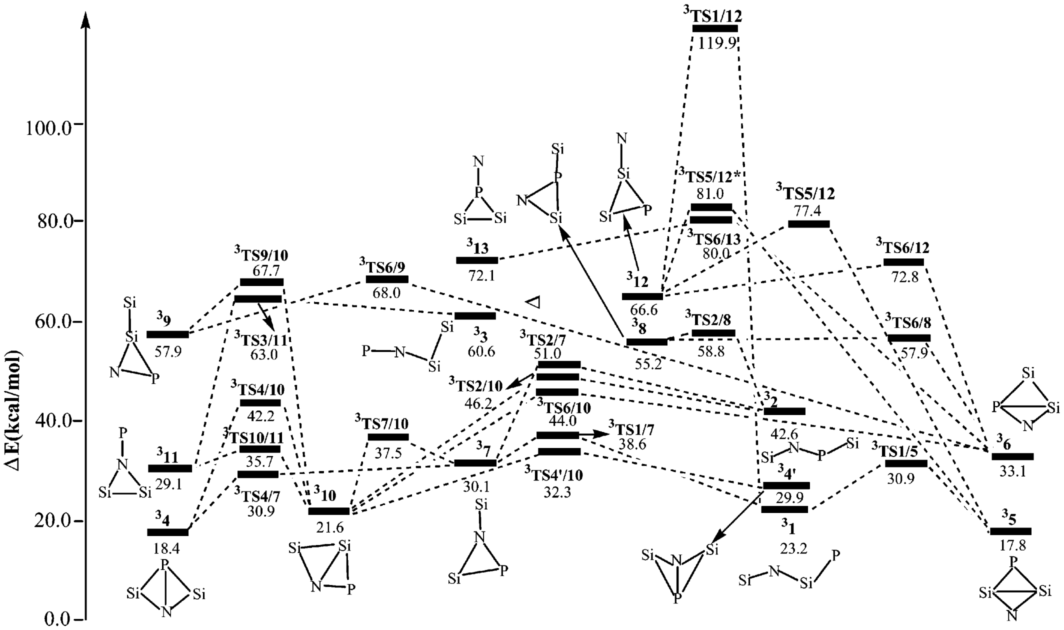

**Figure 6.** Schematic triplet potential-energy surface of $Si_2NP$ at the CCSD(T)/6-311G(2df)//DFT/B3LYP/6-311G(d)+ZPVE level.

**TABLE 3: Relative (kcal/mol) Energies of Dissociation Fragments of the $Si_2NP$ Structures at DFT/B3LYP/6-311G(d) and Single-Point CCSD(T)/6-311g(2df) Levels**[a]

| species | B3LYP[c] | ΔZPVE B3LYP[c] | CCSD(T)[d] //B3LYP[c] | total |
|---|---|---|---|---|
| SiN ($^2\Sigma$) + SiP ($^2\Pi$)[b] | 111.9 | −2.4 | 117.3 | 114.9 |
| SiSi ($^3\Pi_g$) + NP ($^1\Sigma$) | 85. 5 | −1.9 | 83.0 | 81.1 |
| SiSi ($^1\Sigma_g$) + NP ($^1\Sigma$) | 99.3 | −2.0 | 95.5 | 93.5 |
| SiSi ($^3\Pi_g$) + NP ($^3\Pi$) | 178.8 | −2.5 | 182.1 | 179.6 |
| SiSi ($^1\Sigma_g$) + NP ($^3\Pi$) | 192.6 | −2.6 | 194.6 | 192.0 |
| Si ($^1D$) + SiNP ($^3\Sigma$) | 103. 6 | −1.4 | 106.5 | 105.1 |
| Si ($^1D$) + SiNP ($^1\Sigma$) | 122.4 | −1.3 | 122.5 | 121.2 |
| Si ($^3P$) + SiNP ($^3\Sigma$) | 77.4 | −1.4 | 85.7 | 84.3 |
| Si ($^3P$) + SiNP ($^1\Sigma$) | 96.2 | −1.3 | 101.6 | 100.3 |
| N ($^2D$) + SiSiP ($^2\Sigma$) | 218.9 | −3.0 | 214.6 | 211.6 |
| N ($^2D$) + cSiPSi ($^2A_1$) | 186.6 | −2.9 | 175.8 | 172.9 |
| N ($^4S$) + SiSiP ($^2\Sigma$) | 153. 9 | −3.0 | 151.1 | 148.1 |
| N ($^4S$) + cSiPSi ($^2A_1$) | 121.6 | −2.9 | 112.3 | 109.4 |
| Si ($^1D$) + cSiNP ($^1A'$) | 118.9 | −1.6 | 110.7 | 109.1 |
| P ($^2D$) + SiNSi ($^2\Sigma_g$) | 98.8 | −1.6 | 103.5 | 101.9 |
| Si ($^3P$) + cSiNP ($^1A'$) | 92.7 | −1.6 | 89.8 | 88.2 |
| P ($^4S$) + SiNSi ($^2\Sigma_g$) | 60.2 | −1.6 | 64.1 | 62.5 |
| P ($^2D$) + SiSiN ($^2\Sigma$) | 184. 6 | −2.3 | 182.4 | 180.1 |
| P ($^2D$) + cSiNSi ($^2A_1$) | 111.7 | −1.7 | 109.5 | 107.8 |
| P ($^4S$) + SiSiN ($^2\Sigma$) | 146.0 | −2.3 | 142.9 | 140.6 |
| P ($^4S$) + cSiNSi ($^2A_1$) | 73.1 | −1.7 | 70.0 | 68.3 |

[a] The symbols in parentheses of the column denote the point group symmetry. [b] The total energies of reference isomer **$^1$1** at the DFT/B3LYP and single point CCSD(T) levels as well as the ZPVE at the DFT/B3LYP level are listed in footnote b of Table 2. [c] The basis set is 6-311G(d) for DFT/B3LYP. [d] The basis set is 6-311G(2df) for CCSD(T).

Si cross-bonding. The linear or chainlike species are neither minima nor thermodynamically and kinetically stable. The title molecule $Si_2NP$ is the first example of such 18-valence electron series containing three higher-row atoms. The linear SiNSiP **$^1$1** and two cyclic cSiNSiP isomers **$^1$4** and **$^1$5** are of interest. In all, with the increasing number of second-row atoms, the cyclic species becomes more important both thermodynamically and kinetically. This can be attributed to the smaller contribution of second-row elements to $\pi$-conjugation than the first-row elements.

The calculated harmonic vibrational frequencies, dipole moments, and rotational constants (in Table 1) can be useful for the laboratory and interstellar detection of the isomers **$^1$1**, **$^1$4**, and **$^1$5**. At the QCISD/6-311G(d) level, their dominant infrared (IR) vibrational bands are 1384 $cm^{-1}$ (the terminal SiN stretch with IR intensity 466 km/mol), 853 $cm^{-1}$ (the peripheral SiN breathing with IR intensity 57 km/mol), and 904 $cm^{-1}$ (65 km/mol), respectively. Isomer **$^1$4** also has a shoulder band at 440 $cm^{-1}$ associated with the peripheral SiP stretch with the IR intensity 42 km/mol. The dipole moment of the linear SiNSiP **$^1$1** is rather large as 5.4384 D, indicating that it is very promising for radio astronomical detection. The cyclic isomer **$^1$4** still has a considerable dipole moment 1.4566 D. Isomer **$^1$5** has an almost zero dipole moment 0.3305 D, and its characterization can be based on its infrared spectrum.

## 4. Conclusions

To deepen the understanding of the doping effect of the 18-valence electron series AA′BB′ (A, A′ for group IV; B, B′ for group V), we theoretically studied in detail the $Si_2NP$ potential energy surface. Although it contains three second-row atoms, the linear isomer SiNSiP **$^1$1** with a formal valence structure |Si=N−Si≡P| is energetically very low-lying and is almost isoenergetic with the puckered cSiNSiP with crossed N−P bonding **$^1$4**. The third low-lying planar form cSiNSiP with crossed Si−Si bonding **$^1$5** is just 3.3 kcal/mol higher than **$^1$1**. Isomer **$^1$1** is of particular interest because no stable Si≡P triply bonded species have been known experimentally. This also represents the first consideration of the 18e-AA′BB′ series containing three higher-row atoms.

**Acknowledgment.** This work is supported by the National Natural Science Foundation of China (Nos. 29892168, 20073014, 20103003), Doctor Foundation of Educational Ministry, Foundation for University Key Teacher by the Ministry of Education and Key Term of Science and Technology by the Ministry of Education of China, Excellent Young Teacher Foundation of Ministry of Education of China, and Excellent Young People Foundation of Jilin Province, and Key Teacher Innovation

Foundation of Universities of Heilongjiang Province. The authors are greatly thankful to the reviewers' invaluable comments.

## References and Notes

(1) (a) Winnewisser, G. *J. Mol. Struct.* **1997**, *408/409*, 1. (b) McCarthy, M. C.; Apponi, A. J.; Thaddeus, P. *J. Chem. Phys.* **1999**, *110*, 10645. (c) Apponi, A. J.; McCarthy, M. C.; Gottlieb, C. A.; Thaddeus, P. *J. Chem. Phys.* **1999**, *111*, 3911.

(2) (a) Ito, H.; Suzuki, K.; Kondow, T.; Kuchitsu, K. *Chem. Phys. Lett.* **1993**, *208*, 328. (b) Elhanine, M.; Hanoune, B.; Guelachvili, G.; Amiot, *C. J. Phys.* (*Fr*.) **1992**, *2*, 931. (c) Naulin, C.; Costes, M.; Moudden, Z.; Ghanem, N.; Dorthe, G. *Chem. Phys. Lett.* **1993**, *202*, 452. (d) Bruna, P. J.; Dohmann, H.; Peyerimhoff, S. *Can. J. Phys.* **1984**, *62*, 1508. (e) Lembke, R. R.; Ferrante, R. F.; Weltner, Jr. W. *J. Am. Chem. Soc.* **1977**, *99*, 416. (f) Cai, Z. L.; Wang, Y. F.; Xiao, H. M. *J. Chem. Soc. Faraday Trans.* **1992**, *88*, 1611. (g) Ornellas, F. R.; Iwata, S. *J. Phys. Chem*. **1996**, *100*, 10919. (h) Goldberg, N.; Iraqi, M.; Schwarz, H.; Boldyrev, A.; Simons, J. *J. Phys. Chem.* **1994**, *101*, 2871. (i) Davy, R. D.; Schaefer, H. F. *Chem. Phys. Lett.* **1996,** *255*, 171.

(3) Boldyrev, A. I.; Simons, J. *J. Phys. Chem.* **1993**, *97*, 6149. (b) Chong, D. P. *Chem, Phys. Lett.* **1994**, *220*, 102. (c) Davy, R. D.; Schaefer, H. F. *Chem. Phys. Lett*. **1996**, *255*, 171. (d) Elorza, J. M.; Ugalde, J. M. *Can. J. Chem*. **1996**, *74*, 2476. (e) Zhong, S -J.; Liu, C.-W. *J. Mol. Struct*. (*THEOCHEM*) **1997**, *392*, 125.

(4) (a) Brotherton, T. K.; Lynn, J. W. *Chem. Rev.* **1959**, *59*, 84. (b) Ciganek, E., Linn, W. J., Webster, O. W., Rappoport, H., Eds. *The Chemistry of the Cyano Group*, Wiley: London, 1970; p 423, and references therein. (c) Scheller, M. K.; Cederbaum, L. S.; Tarantelli, F. *J. Am. Chem. Soc.* **1990**, *112*, 9484. (d) Ding, Y. H.; Li, Z. S.; Huang, X. R.; Sun, C. C. *J. Chem. Phys.* **2000**, *113*, 1745, and references therein.

(5) (a) Ding, Y. H.; Li, Z. S.; Huang, X. R.; Sun, C. C. *Theor. Chem. Acc.* **2001**, *107*, 1. (b) Pham-Tran, N. N.; Hajgato, B.; Veszpremi, T. et al. *Phys. Chem. Chem. Phys.* **2001**, *3*, 1588. (c) Copper, T. A.; Kroto, H. W.; Nixon, J. F.; Ohashi, O. *J. Chem. Soc. Chem. Commun.* **1980**, *333*. (d) Murckett-St, Laurent J. C. T. R.; Copper, T. A.; Kroto, H. W.; Nixon, J. F.; Ohashi, O.; *J. Mol. Struct*. **1982,** *79*, 215. (e) Bizzocchi, L.; Esposti, C. D.; Botschwina, P. *J. Chem. Phys.* **2000**, *113*, 1465.

(6) Ding, Y. H.; Li, Z. S.; Huang, X. R.; Sun, C. C. *Chem.-Eur. J.* **2001**, *7*, 1539.

(7) Ornellas, F. R.; Iwata, S. *J. Phys. Chem.* **1996**, *100*, 16155.

(8) Huang, X. R.; Ding, Y. H.; Li, Z. S.; Sun, C. C. *J. Phys. Chem. A* **2000**, *104*, 8765.

(9) Frisch, M. J.; Trucks, G. W.; Schlegel, H. B.; Scuseria, G. E.; Robb, M. A.; Cheeseman, J. R.; Zakrzewski, V. G.; Montgomery, J. A., Jr.; Stratmann, R. E.; Burant, J. C.; Dapprich, S.; Millam, J. M.; Daniels, A. D.; Kudin, K. N.; Strain, M. C.; Farkas, O.; Tomasi, J.; Barone, V.; Cossi, M.; Cammi, R.; Mennucci, B.; Pomelli, C.; Adamo, C.; Clifford, S.; Ochterski, J.; Petersson, G. A.; Ayala, P. Y.; Cui, Q.; Morokuma, K.; Malick, D. K.; Rabuck, A. D.; Raghavachari, K.; Foresman, J. B.; Cioslowski, J.; Ortiz, J. V.; Stefanov, B. B.; Liu, G.; Liashenko, A.; Piskorz, P.; Komaromi, I.; Gomperts, R.; Martin, R. L.; Fox, D. J.; Keith, T.; Al-Laham, M. A.; Peng, C. Y.; Nanayakkara, A.; Gonzalez, C.; Challacombe, M.; Gill, P. M. W.; Johnson, B. G.; Chen, W.; Wong, M. W.; Andres, J. L.; Head-Gordon, M.; Replogle, E. S.; Pople, J. A. *Gaussian 98*, revision A.6; Gaussian, Inc.: Pittsburgh, PA, 1998.

(10) The comparative bond lengths of $SiH_3N_2$, $SiH_3P_2$, $SiH_3SiH_3$, $PH_2NH_2$, $SiH_2NH$, HSiP are calculated at the B3LYP/6-311G(d) and B3LYP/6-311G(d, p) (for H-containing species) levels.

(11) In ref 7 of $Si_2N_2$, the kinetic stabilities of isomers were not considered. The isomer cSiNSiN with Si−Si cross-bonding was not located.